Journal of Alloys and Compounds 509 (2011) 185–189

Contents lists available at ScienceDirect

Journal of Alloys and Compounds

journal homepage: www.elsevier.com/locate/jallcom

Spectroscopic properties of Pr^{3+}:$SrMoO_4$ crystal

Jiafeng Cao[b], Yan Wang[a], Xinghua Ma[b], Jianfu Li[a], Zhaojie Zhu[a], Zhenyu You[a], Fugui Yang[b], Chengli Sun[b], Ting Cao[b], Yuexia Ji[b], Chaoyang Tu[a,*]

[a] Key Laboratory of Photoelectric Materials Chemistry and Physics of CAS, Fujian Institute of Research on the Structure of Matter, Chinese Academy of Sciences, Fuzhou, Fujian 350002, China
[b] Graduate School of Chinese Academy of Sciences, Beijing 100039, China

ARTICLE INFO

Article history:
Received 23 June 2010
Received in revised form 1 September 2010
Accepted 4 September 2010
Available online 17 September 2010

PACS:
42.70.Hj
78.20.–e

Keywords:
Pr^{3+}:$SrMoO_4$ crystal
Spectroscopic properties
J–O theory analysis

ABSTRACT

A Pr^{3+}-doped $SrMoO_4$ single crystal has been grown successfully by the Czochralski technique. The absorption spectra, fluorescence spectra, and fluorescence decay curves have been measured at room temperature. The spectroscopic parameters, including spectroscopic parameters Ω_t (t = 2,4,6), radiative transition probabilities, radiative lifetimes and branching ratios were determined according to the standard and modified Judd–Ofelt theories. The stimulated emission cross-sections, the fluorescence lifetimes and the quantum efficiency of Pr^{3+} ions in $SrMoO_4$ were obtained. This study implies that Pr^{3+}:$SrMoO_4$ is an attractive candidate for solid-state laser medium.

1. Introduction

The trivalent praseodymium ion Pr^{3+} has been found to be an attractive ion due to its intricate energy level scheme with various energy gaps and wide emission spectra extending from ultraviolet (UV) to mid-infrared (MIR) regions. Praseodymium ions in crystals present good applications in upconversion [1], fiber amplifiers [2] and red and blue laser [3,4].

$SrMoO_4$ crystal is one excellent laser crystal host [5] due to its good thermal and chemical stability. It belongs to the scheelite ($CaWO_4$) family with the space group of I41/a and the cell parameters as follows: a = 5.394 Å, b = 5.394 Å, c = 12.017 Å [6,7]. The melting point of $SrMoO_4$ is 1328 °C and it melts congruently. Thus large size Pr^{3+}:$SrMoO_4$ single crystal can be obtained by the Czochralski method.

In this work, the standard and modified Judd–Ofelt theories [8,9] have been applied to analyze the polarized absorption spectra to determine the spectroscopic parameters of the Pr^{3+}:$SrMoO_4$ crystal. The emission spectra and the fluorescence decay curve were also obtained at room temperature, and the fluorescence lifetimes for $^3P_0 \rightarrow {}^3H_4$ and $^1D_2 \rightarrow {}^3F_4$ transitions have been determined.

2. Experimental procedure

The Pr^{3+}:$SrMoO_4$ compounds were synthesized by solid-state reaction, and the raw materials were: MoO_3 (analytical grade), $SrCO_3$ (analytical grade) and Pr_2O_3 (4N purity). The starting materials were weighed, mixed up in agate mortar and pressed into cakes. These cakes were slowly heated up to 1080 °C in a platinum crucible for seven days. Then the cakes were put into an iridium-crucible and grown by the Czochralski technique along the c-axis. The pulling and rotation rate were 1.0–1.5 mm/h and 12.0–17.0 rpm, respectively. The crystal was cooled down to the room temperature at a rate of 10.0–35.0 K/h, and the Pr^{3+}-doped $SrMoO_4$ single crystal we obtained is shown in Fig. 1.

Fig. 2 shows the powder XRD pattern of Pr^{3+}:$SrMoO_4$ recorded by Mini Flex II Desktop X-ray Diffractometer using Cu-K_α radiation (λ = 1.54059 Å). Data were collected in the range of 2θ = 5–90° with a scan step of 0.02°. The data analyses were carried out with the aid of the JADE 5.0 software package. All diffraction peaks can be indexed as a tetragonal structure with the space group of I41/a. The lattice parameters were calculated according to the refinement, and the final lattice parameters were achieved with $a = b$ = 5.38969 Å, c = 12.00721 Å, with volume unit cell of 348.79 Å^3. These values are in agreement with the standard JCPDS card of $SrMoO_4$ (85–0809).

The concentration of praseodymium ions in the crystal was measured to be 0.34 wt% by the inductively coupled plasma-atomic emission spectrometry (ICP-AES) method and the corresponding Pr^{3+} concentration is 6.8293×10^{19} ions/cm^3.

The sample used for spectroscopic measurements was optically polished to flat and parallel faces with the thickness of 2.0 mm. Room temperature polarized absorption spectra of this crystal were obtained by a Perkin-Elmer UV-VIS-NIR spectrometer Lambda-900. The emission spectra and the decay curves of the crystal were

* Corresponding author. Tel.: +86 591 8371 1368; fax: +86 591 8371 4946.
E-mail address: tcy@fjirsm.ac.cn (C. Tu).

0925-8388/$ – see front matter © 2010 Elsevier B.V. All rights reserved.
doi:10.1016/j.jallcom.2010.09.029

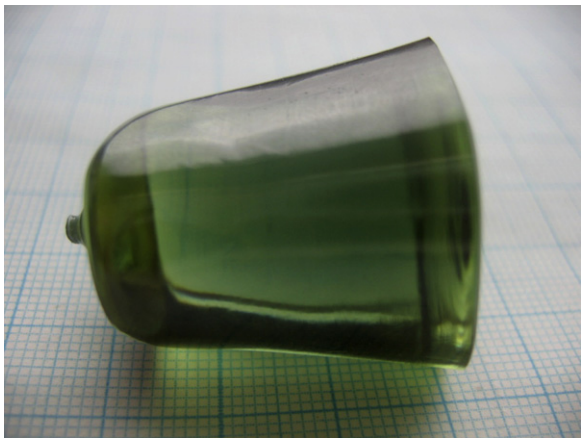

Fig. 1. Picture of the Pr^{3+}:$SrMoO_4$ crystal.

recorded at room temperature by an Edinburgh Instrument FLS920 spectrophotometer.

3. Results and discussion

3.1. Absorption spectroscopy and Judd–Ofelt analysis

The room temperature polarized absorption spectra of Pr^{3+}:$SrMoO_4$ were represented in Fig. 3 in the range of 300–2300 nm. The terminal levels of each transition from the $^3H_4$ ground state were assigned according to the Pr^{3+} scheme of levels in familiar oxide hosts. It can be found that these bands are related to the transitions between the ground $^3H_4$ level and the excited $^3P_{0-2}$, $^1D_2$, $^1F_{2-4}$ levels. Fig. 3 shows that Pr^{3+}:$SrMoO_4$ crystal has strong absorption in two bands with peaks at 487 nm and 592 nm, corresponding to the $^3H_4 \rightarrow {}^3P_0$ and $^3H_4 \rightarrow {}^1D_2$ transitions, respectively.

The Judd–Oflet (J–O) theory [8,9] has been widely used to analyze the spectroscopic properties of rare-earth ions doped host materials. For the slight contributions to the line strengths of Pr^{3+} ions, the magnetic dipole transitions are not taken into account in the J–O calculations, and only the electric dipole transitions are considered. According to the standard J–O theory, the experimental

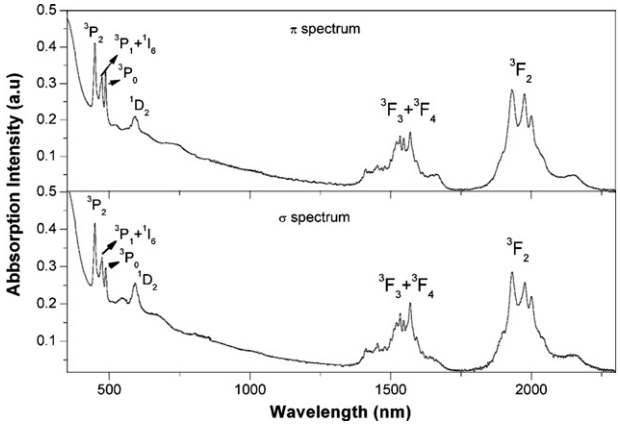

Fig. 3. Polarized room temperature absorption spectra of Pr^{3+}:$SrMoO_4$.

line strength $S_{exp}(J–J')$ can be calculated by the following formula [10]:

$$S_{exp}(J–J') = \frac{3ch(2J+1)}{8\pi^3 N_0 \bar{\lambda} e^2} \frac{\Gamma_\pi + 2\Gamma_\sigma}{x_\pi + 2x_\sigma} \quad (1)$$

here N_0 is the Pr^{3+} concentration in the crystal, c is the vacuum speed of light, h is Planck's constant, J is the total angular momentum of the ground state ($J = 4$ in Pr^{3+}), λ is the mean wavelength of the absorption band, $\chi_{\sigma,\pi} = (n^2_{\sigma,\pi} + 2)^2/9n_{\sigma,\pi}$ is the Lorentz local field correction for the refractivity of the medium, n_σ and n_π are the values of ordinary and extraordinary refractive indices of the $SrMoO_4$ crystal, which can be obtained by [11]:

$$n_o^2 = 4.1366 + \frac{76,882}{\lambda^2 - 36,374}$$
$$n_e^2 = 4.1569 + \frac{76,365}{\lambda^2 - 46,482}, \quad (2)$$

and the results are shown in Table 1.

Γ is the integrated absorbance for each absorption band, which can be obtained by the following equation:

$$\Gamma = \frac{\int D(\lambda)d\lambda}{L \log e} = \frac{2.303 \int D(\lambda)d\lambda}{L}, \quad (3)$$

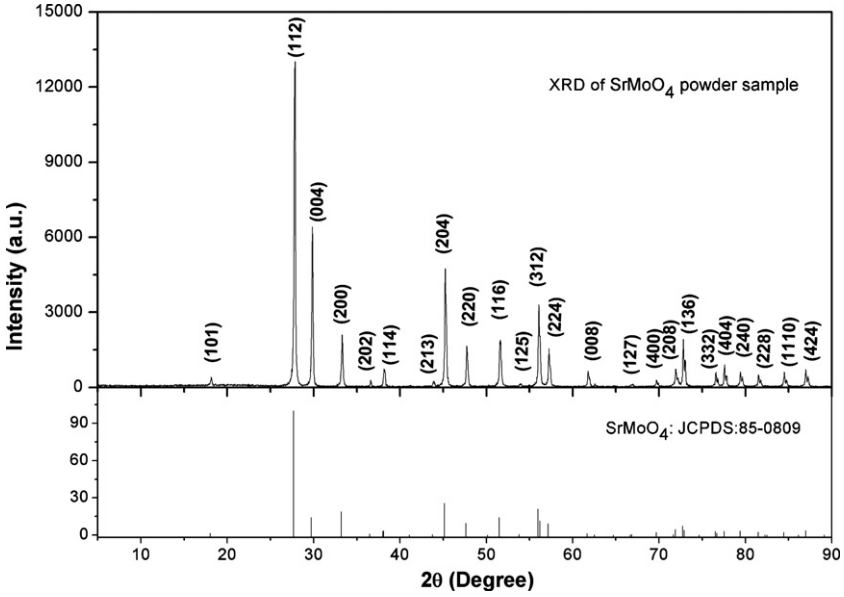

Fig. 2. X-ray diffraction pattern of $SrMoO_4$ powder sample and the standard JCPDS card of $SrMoO_4$ (85–0809).

Table 1
The values of ordinary and extraordinary refractive indices.

λ (nm)	n_σ	n_π
450	2.1446	2.1555
472	2.1328	2.1424
488	2.1255	2.1343
593	2.0930	2.0993
1538	2.0420	2.0469
2024	2.0385	2.0435

where L is the sample thickness ($L = 0.20$ cm) and $D(\lambda)$ is the measured optical density as a function of wavelength.

The measured line strengths were used to obtain J–O intensity parameters Ω_t ($t = 2,4,6$) by fitting the following set of equations:

$$S_{calc}(J \to J') = \Omega_2 U^{(2)}_{JJ'_n} + \Omega_4 U^{(4)}_{JJ'_n} + \Omega_6 U^{(6)}_{JJ'_n} \quad (4)$$

$$U^{(t)}_{JJ'} = \left|\left\langle f^N \Psi J \left\| U^{(t)} \right\| f^N \Psi J' \right\rangle\right|^2, \quad (t = 2, 4, 6) \quad (5)$$

here $U^{(t)}_{JJ'}$ ($t = 2,4,6$) are the reduced matrix elements of tensor operators, given in Ref. [12]. When two absorption manifolds overlapped, the squared matrix element was taken to be the sum of the corresponding squared matrix elements. The effective Judd–Ofelt intensity parameters for Pr^{3+}:$SrMoO_4$ were obtained by combining Eqs. (4) and (5). And the integrate absorbance and electrical dipole line strengths are shown in Table 2.

The root-mean-square deviation between the experimental and calculated strengths was obtained by:

$$\mathrm{rm}\Delta S = \sqrt{\sum_{i=1}^{N} \frac{(S_{\mathrm{exp}} - S_{calc})^2}{N-3}}, \quad (6)$$

where N ($N = 6$ in our case) is the number of absorption bands.

After a least-square fitting of S_{mea} to S_{calc}, the three J–O intensity parameters we obtained were 16.56×10^{-20} cm^2, 6.09×10^{-20} cm^2 and 3.74×10^{-20} cm^2, respectively, and the value of rmΔS was calculated to be 1.491×10^{-20} cm^2. We find high values of J–O intensity parameters of Pr^{3+}:$SrMoO_4$. But we also find large deviation between experimental and calculated data by using standard J–O theory. In order to overcome errors using this theory, we tried to avoid the $^3H_4 \to {}^3P_2$ transition, and the three J–O intensity parameters we obtained were $\Omega_2 = 16.641 \times 10^{-20}$ cm^2; $\Omega_4 = 6.174 \times 10^{-20}$ cm^2; $\Omega_6 = 3.479 \times 10^{-20}$ cm^2. As shown in Table 3, there are still large errors between experimental and calculated data. So in the following analyses, we use modified J–O theory to avoid wrong results.

Modified J–O theory is one method to improve the reliability of the J–O parameters which has been proposed by Dunina et al. [13]. This theory improved calculated line strengths with an additional introduced parameter. The modified line strength formula is expressed as follows:

$$S_{calc} = S_{calc}(\mathrm{standard}) \times \left[1 + \frac{E_i - 2E^0_{\mathrm{f}}}{E_{5\mathrm{d}} - E^0_{\mathrm{f}}}\right] \quad (7)$$

here S_{calc} (standard) is defined in Eq. (4), E_i is the energy of transition, $E_{5\mathrm{d}}$ is the energy of the lowest 4f5d state, and E^0_{f} is the average energy over the $4f^2$ states. The values of E^0_{f} and $E_{5\mathrm{d}}$ are 10 000 and 60 000 cm^{-1} [14] in our case.

On the basis of the modified J–O theory, both calculations with and without the $^3H_4 \to {}^3P_2$ transition were obtained, as shown in Table 3. The final experimental J–O parameters of Pr^{3+}:$SrMoO_4$ we obtained were $\Omega_2 = 10.066 \times 10^{-20}$ cm^2; $\Omega_4 = 6.567 \times 10^{-20}$ cm^2; $\Omega_6 = 1.979 \times 10^{-20}$ cm^2, which shows that Pr^{3+}:$SrMoO_4$ has higher value compared with other crystal hosts (shown in Table 4).

Then the radiative decay rates $A(J \to J')$ can be obtained by the following expression:

$$A(J \to J') = \frac{64\pi^4 e^2}{3h(2J+1)\overline{\lambda^3}} \frac{n(n^2+2)^2}{9} \times \sum_{t=2,4,6} \Omega_t \left|\left\langle (S,L)J \left\| U^t \right\| (S',L')J' \right\rangle\right|^2 \times \left[1 + \frac{E_i - 2E^0_{\mathrm{f}}}{E_{5\mathrm{d}} - E^0_{\mathrm{f}}}\right] \quad (8)$$

here U^t ($t = 2,4,6$) are the reduced matrix elements of tensor operators, given in Ref. [17].

The fluorescent branching ratio is expressed by the following equation [18]:

$$\beta_{JJ'} = \frac{A(J \to J')}{\sum_{J'} A(J \to J')}. \quad (9)$$

And the radiative lifetime is:

$$\tau_{rad} = \frac{1}{\sum_{J'} A(J \to J')}. \quad (10)$$

According to modified J–O theory, the values of $A_{JJ'}$, $\beta_{JJ'}$ and τ_{rad} were obtained and shown in Table 5.

Table 2
The integrate absorbance and electrical dipole line strengths.

Excited states	λ (nm)	Γ (nm/cm)			Line strength (10^{-20} cm^2)	
		σ	π	$\Gamma_\pi + 2\Gamma_\sigma$	S_{mea}	S_{calc}
$^3P_2$	450	21.75	21.68	65.18	3.045	0.727
$^3P_1 + {}^1I_6$	472	12.95	12.83	38.73	1.725	1.598
$^3P_0$	488	6.34	8.83	21.51	0.927	1.052
$^1D_2$	593	15.22	9.58	40.02	1.255	0.341
$^3F_3 + {}^3F_4$	1538	192.82	193.45	579.09	7.916	8.235
$^3F_2$	2024	358.33	377.82	1094.48	11.368	11.323

Table 3
J–O parameters and the corresponding root-mean-square deviations for the Pr^{3+}:$SrMoO_4$ crystal obtained by different methods.

J–O parameters (10^{-20} cm^2)	The standard J–O theory		The modified J–O theory	
	With $^3H_4 \to {}^3P_2$	Without $^3H_4 \to {}^3P_2$	With $^3H_4 \to {}^3P_2$	Without $^3H_4 \to {}^3P_2$
Ω_2	16.56	16.641	10.015	10.066
Ω_4	6.09	6.174	6.478	6.567
Ω_6	3.74	3.479	2.201	1.979
rmΔS	1.491	0.782	0.144	0.071

Table 4
Comparison of the Judd–Ofelt parameters of Pr^{3+}-doped crystals.

Crystals	Ω_2 (10^{-20} cm^2)	Ω_4 (10^{-20} cm^2)	Ω_6 (10^{-20} cm^2)	References
Pr^{3+}:$SrMoO_4$	10.066	6.567	1.979	This work
$Ca_5(PO_4)_3F$	0.32	1.59	3.82	[15]
YAG	0	12.2	8.72	[16]
$NaBi(MoO_4)_2$	9.8	12.8	1.3	[15]

Table 5
Calculated radiative transition rates, branching ratios radiative lifetimes and oscillator strength for different transition levels of Pr^{3+}:$SrMoO_4$ crystal.

Transition	Wavelength (nm)	A (s^{-1})	β	τ (μs)
$^3P_0 \rightarrow {}^3H_4$	489	40,180	0.372	9.252
$\rightarrow {}^3H_5$	532	0	0	
$\rightarrow {}^3H_6$	619	2882	0.027	
$\rightarrow {}^3F_2$	647	53,230	0.493	
$\rightarrow {}^3F_3$	697	0	0	
$\rightarrow {}^3F_4$	732	9185	0.085	
$\rightarrow {}^1G_4$	924	2558	0.024	
$\rightarrow {}^1D_4$	2746	46.711	0.00043	
$^1D_2 \rightarrow {}^3H_4$	592	994.39	0.099	99.451
$\rightarrow {}^3H_5$	659	46.855	0.00466	
$\rightarrow {}^3H_6$	822	833.598	0.083	
$\rightarrow {}^3F_2$	885	1040	0.103	
$\rightarrow {}^3F_3$	1001	466.422	0.046	
$\rightarrow {}^3F_4$	1058	5399	0.537	
$\rightarrow {}^1G_4$	1442	1274	0.127	

3.2. Fluorescence spectroscopy and stimulated emission cross-sections

The room temperature polarized emission spectra of Pr^{3+}:$SrMoO_4$ excited by 448 nm are shown in Fig. 4. Several emission bands with peaks at 619 nm, 647 nm and 732 nm can be found in Fig. 4, corresponding to the emissions from the metastable ^3P_j (j = 0–2) manifolds. The most intensive emission locates around 647 nm, which is considered to be the transition $^3P_0 \rightarrow {}^3F_2$. Fig. 5 shows the room temperature polarized emission spectra of Pr^{3+}:$SrMoO_4$ excited by 592 nm, and two strong emission bands centered at 890 nm and 1058 nm were recorded, corresponding to the transitions $^1D_2 \rightarrow {}^3F_2$ and $^1D_2 \rightarrow {}^3F_4$, respectively.

The emission cross-section is an important parameter responsible for the potential laser performance. According to the Fuchtbauer–Ladengurg (F–L) formula [19], the emission cross-section can be expressed by the following equation:

$$\sigma_{em}(\lambda) = \frac{\lambda^5 \beta}{8\pi c n^2 \tau_r} \frac{3I_{\sigma,\pi}(\lambda)}{\int [2I_\sigma(\lambda) + I_\pi(\lambda)]\lambda \, d\lambda}, \quad (11)$$

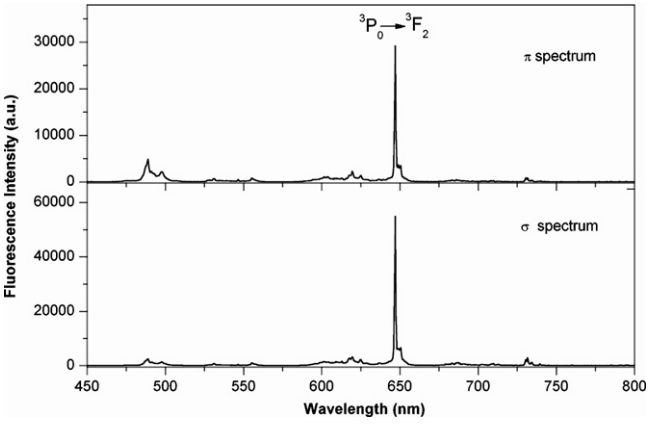

Fig. 4. Visible fluorescence spectra of Pr^{3+}:$SrMoO_4$ crystal excited by 448 nm pumping.

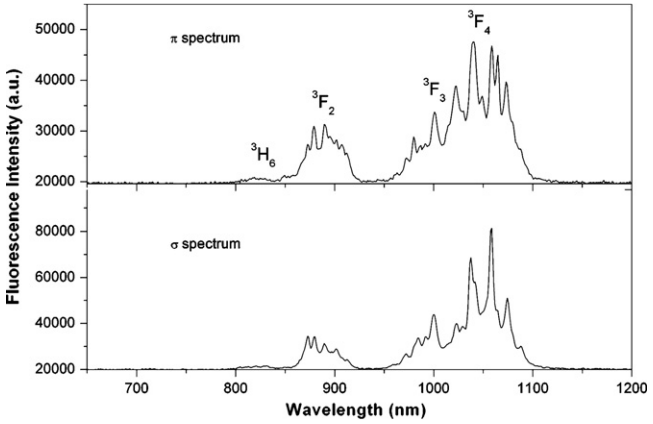

Fig. 5. Infrared fluorescence spectra of Pr^{3+}:$SrMoO_4$ crystal excited by 592 nm pumping.

where $I_{\sigma,\pi}$ (λ) is the experimental emission intensity for σ and π polarization spectra as a function of λ.

According to the above equation, the calculated cross-sections of the transition $^3P_0 \rightarrow {}^3F_2$ are 77.13×10^{-20} cm^2 (σ) and 41.03×10^{-20} cm^2 (π). The calculated cross-sections of the $^1D_2 \rightarrow {}^3F_2$ and $^1D_2 \rightarrow {}^3F_4$ transitions are 0.092×10^{-20} cm^2 (σ), 0.0717×10^{-20} cm^2 (π) and 0.955×10^{-20} cm^2 (σ), 0.429×10^{-20} cm^2 (π), respectively.

3.3. Fluorescence lifetimes and quantum efficiency

The decay curves of the crystal recorded at 488 nm and around 1060 nm were measured at room temperature by an Edinburgh Instrument FLS920 spectrophotometer. Figs. 6 and 7 show the decay curves excited by 448 nm and 592 nm pumping at room temperature, corresponding to the $^3P_0 \rightarrow {}^3H_4$ and $^1D_2 \rightarrow {}^3F_4$ transitions. It can be found in Fig. 6 that the curve displays a single exponential behavior and the fluorescence lifetime of the $^3P_0$

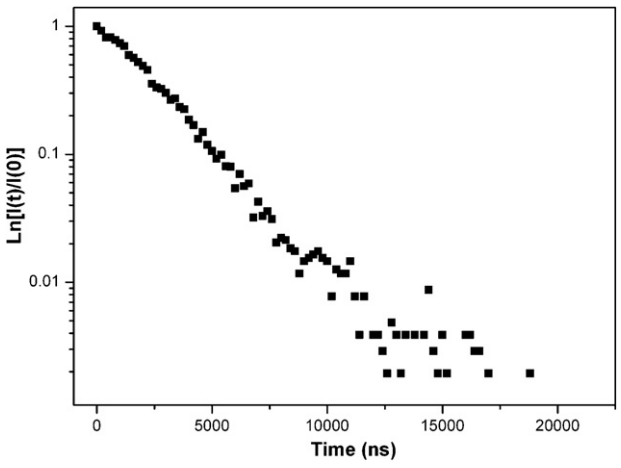

Fig. 6. Room temperature luminescence decay curve at 488 nm excited by 448 nm pumping.

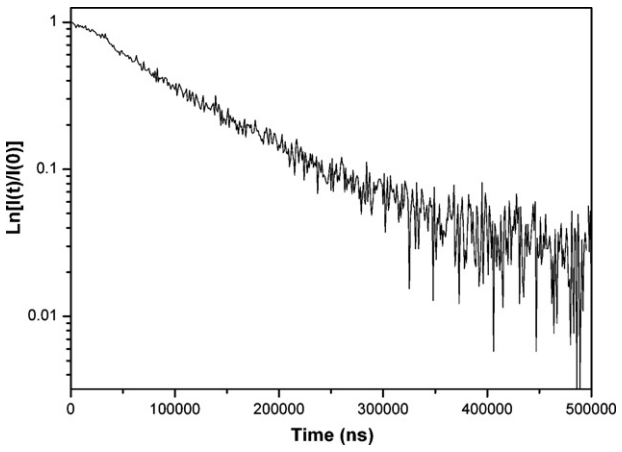

Fig. 7. Room temperature luminescence decay curve at 1060 nm excited by 592 nm pumping.

manifold is estimated to be 2.63 μs, which can be compared with Pr^{3+}:$NaBi(WO_4)_2$: 1.2 μs [15] and Pr^{3+}:$CaNb_2O_6$: less than 1.0 μs [20]. We found short fluorescence lifetime of $^3P_0$ level for Pr^{3+}:$SrMoO_4$ crystal, but the product of the emission cross-section σ and the mean fluorescence lifetime τ (2.03×10^{-18} cm^2 μs for π-polarization and 1.08×10^{-18} cm^2 μs for σ-polarization) is bigger than other crystals such as Pr^{3+}:$NaY(MoO_4)_2$ (0.89×10^{-18} cm^2 μs for π-polarization and 0.79×10^{-18} cm^2 μs for σ-polarization) [21].

Fig. 7 shows the luminescence decay curve of the $^1D_2 \rightarrow {}^3F_4$ transition, and lifetime measurements show a single exponential for $^1D_2$ level too. This suggests that no energy transfer processes involving the $^1D_2$ level are present in this system and the mean value of the fluorescence lifetime was estimated to be 92.88 μs, which can be compared with Pr^{3+}:YAP: 28 μs [22]. The quantum efficiency was calculated to be 93.39% according the equation $\eta = \tau_f/\tau_r$ for the $^1D_2 \rightarrow {}^3F_4$ transition, which is higher than Pr^{3+}:YAG: 90% [16]. The result demonstrates that Pr^{3+}:$SrMoO_4$ crystal has high luminescent quantum efficiency.

4. Conclusion

Pr^{3+}:$SrMoO_4$ single crystal was grown by the Czochralski method, and the spectroscopic properties of the Pr^{3+} ions in $SrMoO_4$ crystal were reported. The absorption spectra were analyzed by the standard Judd–Ofelt theory, and the accurate results were obtained by modified J–O theory. Three J–O intensity parameters we obtained were $\Omega_2 = 10.066 \times 10^{-20}$ cm^2, $\Omega_4 = 6.567 \times 10^{-20}$ cm^2 and $\Omega_6 = 1.979 \times 10^{-20}$ cm^2, respectively.

The emission cross-sections were estimated by the F–L formula. The fluorescence lifetimes were determined, and the quantum efficiency of the $^1D_2 \rightarrow {}^3F_4$ transition was calculated to be 93.39%. Results of this work demonstrate that the Pr^{3+}:$SrMoO_4$ single crystal may be a good prospective material for solid-state laser medium.

Acknowledgements

This work was supported by Major Projects from FJIRSM (SZD08001-2 and SZD09001), Fund of Key Laboratory of Optoelectronic Materials Chemistry and Physics and Chinese Academy of Sciences (2008DP173016), National Nature Science Foundation of China (No. 50902129, 61078076), Science and Technology Plan Major Project of Fujian Province of China (Grant No. 2010I0015) and Fund of Research Center of Laser Technology Integration and Application Engineering Technology of Haixi Industrial Technology Research Institute (2009H2009).

References

[1] E. Osiac, E. Heumann, G. Hubert, S. Kuck, E. Sani, A. Toncelli, M. Tonelli, Appl. Phys. Lett. 82 (2003) 3832.
[2] R.C. Schimmel, A.J. Faber, H. de Waardt, R.G.C. Beerkens, G.D. Khoe, J. Non-Cryst. Solids 284 (2001) 188.
[3] A. Richter, E. Heumann, E. Osiac, G. Huber, W. Seelert, A. Diening, Opt. Lett. 9 (2004) 2638.
[4] L. Esterowitz, R. Allen, M. Kruer, F. Bartoli, L.S. Goldberg, H.P. Jenssen, A. Linz, V.O. Nicolai, J. Appl. Phys. 48 (1977) 650.
[5] A.A. Kaminskii, S.N. Bagaev, K. Ueda, K. Takaichi, H.J. Eichler, Crystallogr. Rep. 47 (2002) 653.
[6] E. Guermen, E. Daniels, J.S. King, J. Chem. Phys. 55 (1971) 1093.
[7] D. Errandonea, R.S. Kumar, X. Ma, C. Tu, J. Solid State Chem. 181 (2008) 355.
[8] G.S. Ofelt, J. Chem. Phys. 37 (1962) 511.
[9] B.R. Judd, Phys. Rev. 127 (1962) 750.
[10] D. Jaque, O. Enguita, U. Caldino, M.O. Ramirez, J. Garcia Sole, J. Appl. Phys. 90 (2001) 561.
[11] X. Ma, Z. You, Z. Zhu, J. Li, B. Wu, Y. Wang, C. Tu, J. Alloys Compd. 465 (2008) 406.
[12] W.T. Carnall, P.R. Fields, K. Rajnak, J. Chem. Phys. 49 (1968) 4424.
[13] E.B. Dunina, A.A. Kaminskii, A.A. Kornienko, K. Kurbanov, K.K. Pukhov, Sov. Phys. Solid State 32 (1990) 290.
[14] P. Goldner, F. Auzel, J. Appl. Phys. 79 (1996) 7972.
[15] A. Mendez-Blas, M. Rico, V. Volkov, C. Cascales, C. Zaldo, C. Coya, A. Kling, L.C. Alves, J. Phys.: Condens. Matter 16 (2004) 2139.
[16] M. Malinowski, R. Wolski, W. Wolinski, Solid State Commun. 74 (1990) 17.
[17] P. Babu, C.K. Jayasankar, Physica B 301 (2001) 326.
[18] W.F. Krupke, IEEE J. Quant. Electron. 10 (1974) 450.
[19] B.M. Walsh, N.P. Barnes, B. Di Bartolo, J. Appl. Phys. 83 (1998) 2772.
[20] L. Macalik, M. Maczka, J. Hanuza, P. Godlewska, P. Solarz, W. Ryba-Romanowski, A.A. Kaminskii, J. Alloys Compd. 451 (2008) 234.
[21] X. Lu, Z. You, J. Li, Z. Zhu, G. Jia, B. Wu, C. Tu, Appl. Phys. B 85 (2006) 585.
[22] G. Ozen, O. Forte, B. Di Bartolo, J.M. Collins, J. Lumin. 125 (2007) 223.